Journal of Molecular Structure 1226 (2021) 129343

Contents lists available at ScienceDirect

Journal of Molecular Structure

journal homepage: www.elsevier.com/locate/molstr

Interaction between dopamine and the $[HPW_{12}O_{40}]^{2-}$Keggin ion–an X-ray and NMR study

Fredric G. Svensson*, Vadim G. Kessler

Department of Molecular Sciences, Swedish University of Agricultural Sciences, Box 7015, 750 07 Uppsala, Sweden

ARTICLE INFO

Article history:
Received 17 July 2020
Revised 20 September 2020
Accepted 25 September 2020
Available online 28 September 2020

Keywords:
Polyoxometalate
Dopamine
Keggin ion
Phosphotungstate

ABSTRACT

A novel complex between the $[HPW_{12}O_{40}]^{2-}$ Keggin ion and the biomolecule dopamine ($C_8H_{11}NO_2$), $[HPW_{12}O_{40}(dop)_2]$ • $4H_2O$ (**1**) was crystallized and structurally characterized by single crystal X-ray diffraction and infrared spectrometry. Dopamine interacts via hydrogen bonding between its ammonium group and a W=O oxygen atom in $[HPW_{12}O_{40}]^{2-}$. NMR analyses (^1H DOSY) suggests that the $[HPW_{12}O_{40}(dop)_2]$ complex dissociates in D_2O.

1. Introduction

Nanoparticles are inevitable in society today. Although they are increasingly present as engineered materials (cosmetics, antibacterials, medicine, etc.), and from human-related pollution such as exhausts, they also have natural origins, such as volcanic eruptions and weathering of rocks and have been around since the very origin of life [1–3]. Nanomaterials, and in particular nanoparticles, are in the same size regime (<100 nm) as the cellular signaling pathways and “molecular factories”; thus they may interfere with biological processes [4]. Alterations in DNA transcription and protein synthesis upon exposure to nanoparticles have been reported [5–7]. This certainly raises concerns about potential health issues, but also holds promise for novel applications within bionanotechnology. For example, the group of Parac-Vogt have demonstrated the potential use of polyoxometalates (POMs) for selective peptide hydrolysis [8,9]. Colloidal sprays of titania nanoparticles have been utilized for promoting scar-healing by increased activation of the coagulation system [10]. A third well-known example is the antibacterial function of silver nanoparticles, sometimes added in sportswear. Thus, the increasing presence of inorganic nanoparticles, both from engineered nanomaterials, from pollution, and in emerging medical applications calls for a better understanding for the interaction between nanoparticles and biomolecules [11]. Polyoxometalates (POMs), typically group V/VI polyanions, provide attractive model systems for nanoparticles. POMs are currently being extensively investigated for their antiviral and antitumor properties, where their biological functions originate from their interference with biomolecules [12]. Several complexes between phosphotungstate, phosphomolybdate, and related hetero-polyoxometalates and amino acids or peptides have been published [13–18]. Eshtiagh-Hosseini and Mirzaei [13] reported several complexes between $P_5W_{30}O_{110}$ and $P_2W_{18}O_{62}$ and the amino acids valine, glycine, and proline. Rominger and coworkers [19] synthesized a number of complexes between phosphotungstate and phosphomolybdate POMs and the glycylglycine dipeptide and arginine. The interactions were found to persist even in solution, as determined by diffusion constants obtained from NMR experiments. Dopamine, a catecholamine, is present in the body as both an important hormone and a neuroregulator [20]. The two vicinal hydroxide groups of catechol are known to form chelates with several metal centers [21], thus dopamine could potentially interact with mineral nanoparticles. There have been a recent interest in hybrid materials based on dopamine, particularly for cancer treatment and production of hybrid materials. Messersmith and co-workers [22] developed a poly-dopamine coating suitable for a wide variety of material surfaces, both organic and inorganic, which could further be functionalized with other organic compounds. Li et al., [23] developed dopamine-genipin nanoparticles loaded with the anticancer bortezomib. The system had a dual therapeutic effect. Laser irradiation of the nanoparticles resulted in the production of reactive oxygen species and at lowered pH (i.e. cytoplasm of cancer cells) the bortezomib drug was released. In another work, dopamine was used to direct the self-assembly of phosphotungstic acid into flowerlike spheres. The spheres, which had a highly hierarchal structure, were evaluated for delivery of

* Corresponding author.
E-mail address: fredric.svensson@slu.se (F.G. Svensson).

https://doi.org/10.1016/j.molstruc.2020.129343

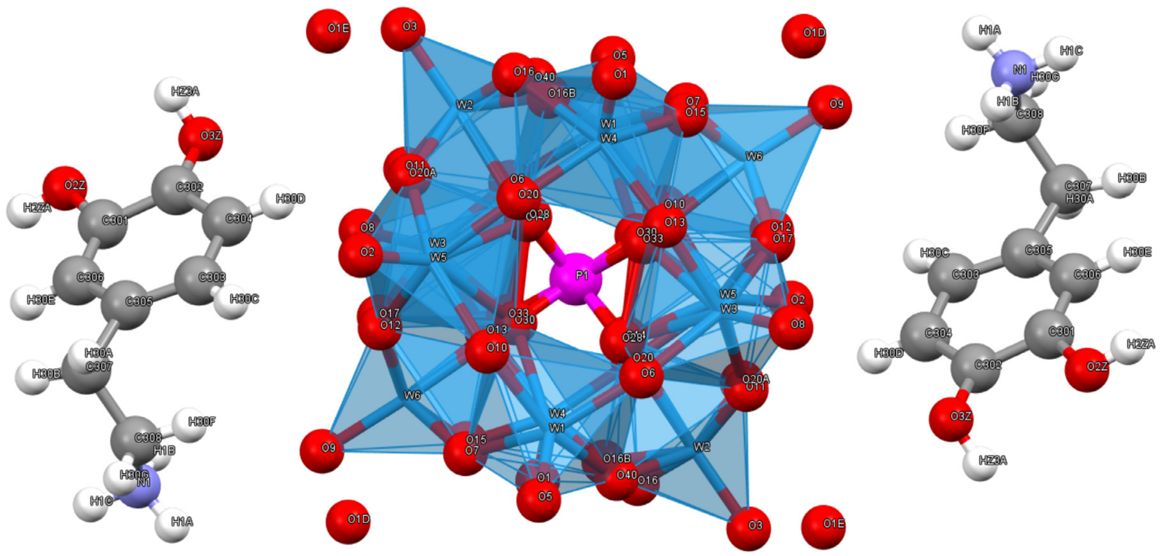

Fig. 1. Molecular structure of **1**. Magenta is phosphorous, blue is tungsten, red is oxygen, grey is carbon, white is hydrogen, and purple is nitrogen. The disorder for O1D is not shown.

anticancer drug doxorubicin with promising results [24]. Due to the broad interest in the interplay between dopamine and metal oxide surfaces, the molecular interaction between dopamine and nanoparticles is of great interest. In this report we have crystallized a complex consisting of dopamine and the $[HPW_{12}O_{40}]^{2-}$ ion. The solid-state structure as determined by single crystal X-ray diffraction and its solution behavior investigated by ^{1}H, ^{31}P, and ^{1}H DOSY NMR are reported.

2. Materials and methods

Phosphotungstic acid hydrate (Sigma-Aldrich) was dissolved in 1 M hydrochloric acid (Sigma-Aldrich). Then, two equivalents of dopamine • HCl (Aldrich) were added. The reaction mixture was left at room temperature and after about two days, orange needle shaped crystals begun to form in flower-like aggregates. X-ray data was collected using a Bruker D8 SMART APEX II CCD diffractometer with graphite monochromator and MoKα radiation (0.71073 Å) at room temperature. The structures were solved and refined in the SHELX 97 program suite. All non-hydrogen atoms were found in the initial solution for both compounds. The crystals of **1** were stable in air for at least a few days without protection.

For NMR analyses, ~20 mg of **1** (washed three times with 1 M HCl followed by three times with MilliQ-water) were dissolved in 600 μL D_2O (99.96%, Eurisotop). All NMR spectra were recorded using a Bruker Avance 600 MHz SmartProbe Spectrometer with Bruker TopSpin version 3.5. Bruker TopSpin version 3.6 was used for data processing and data analysis. The ^{1}H spectra were calibrated against the internal water signal. An 85% H_3PO_4 internal standard was used as calibration for the ^{31}P NMR spectrum. All spectra were recorded at 37 °C. NMR assignments for **1**: ^{1}H NMR δ ppm: 7.05 (s, O**H**), 7.07 (s, N$\mathbf{H}_3$), 6.99 (d, J = 2.00 Hz, C$\mathbf{H}_{arom}$), 6.92 (d, J = 1.95 Hz, C$\mathbf{H}_{arom}$), 6.90 (d, J = 1.99, C$\mathbf{H}_{arom}$), 3.39 (t, J = 7.17 Hz, C$\mathbf{H}_2$) and 3.04 (t, J = 7.17, C$\mathbf{H}_2$). ^{31}P NMR δ ppm: −15.13 ($[\mathbf{P}W_{12}O_{40}]^{3-}$, major), 3 ($[\mathbf{P}W_9O_{34}]^{9-}$, minor).

A PerkinElmer FTIR spectrometer Spectrum-100 was used for infrared spectrometry. Crystals were washed as for the NMR experiments and dried under a desktop lamp. The dried crystals of **1** were grinded in anhydrous KBr (dried at 200 °C overnight), pressed to a pellet and a FTIR spectrum was recorded for 4000–400 cm^{-1} with 1 cm^{-1} resolution and 16 scans per spectrum. A Hitachi TM-1000 electron microscope was used for imaging of the crystals.

3. Results and discussion

3.1. Structural comments

Reaction between $H_3PW_{12}O_{40}$ and dopamine in 1 M hydrochloric acid lead to the formation of **1** (Fig. 1) which is a complex between the phosphotungstate ion and dopamine. It crystallized in the triclinic space group P−1. Detailed crystallographic data is presented in Table 1. Each dopamine molecule has one +1 charge due to the protonated ammonium group. Intermolecular distances, and the W–O–W and W=O bond lengths in the phosphotungstate ion, suggest the remaining hydrogen is located in the POM but not at any specific position, resulting in the proposed structure $[HPW_{12}O_{40}(dop)_2]$ • $4H_2O$. The dopamine molecule interacts via hydrogen bonding between its ammonium group (H1A and H1B) and O9(W6) with distances 2.839 Å and 2.817 Å, respectively. Each asymmetric unit contains two water molecules, one is disordered over two positions (O1D). Short contacts between the other water molecule (O1E) with dopamine (O1E)-HZ3A(O3Z), 3.300 Å, and the POM, O8(W3) and O3(W2), 3.455 Å and 3.754 Å, respectively, indicates hydrogen bonding.

Table 1
Crystallographic data for **1**.

Compound	1
Chemical composition	$C_{16}H_{33}O_{48}N_2PW_{12}$
Formula weight	3260.23
Crystal system	Triclinic
Space group	P-1
R1	0.0675
wR2	0.2003
GooF	1.004
a (Å)	9.768(8)
b (Å)	9.903(8)
c (Å)	15.587(12)
α (°)	71.811(9)
β(°)	77.796(9)
γ (°)	88.582(8)
V (Å^3)	1398.6(19)
T (K)	296
Z	1
Nr. refl.	2486
Data completeness	0.974

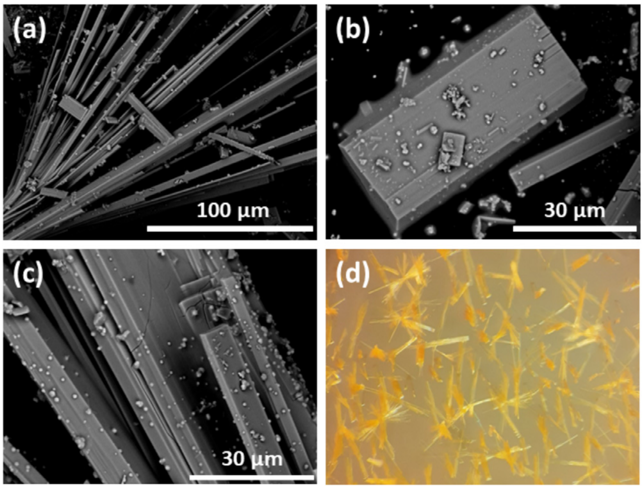

Fig. 2. SEM micrographs of the crystals for compound 1 (a–c) and optical image of crystal aggregates (d).

The surface morphology for crystals of compound **1** was investigated by scanning electron microscopy (SEM), Fig. 2. From Fig. 2d it is visible that the crystals grow flowerlike aggregates, which is also seen in the SEM micrograph (Fig. 2a.). The surfaces are very smooth and the long needles seem to consist of layered sheets according to Fig. 2a and c.

3.2. Infrared spectrometry

A FTIR spectrum of **1** was recorded, Fig. 3. Vibrations at 3556 cm^{-1} and 3366 cm^{-1} are assigned to ν(O–H) and $\nu(NH_3^+)$, respectively. Signals belonging to the aromatic ring of dopamine are found at 1604 cm^{-1} and 1505 cm^{-1} from ν(C=C) and $\nu(C{-}H_{arom})$, respectively. Vibrations for $[PW_{12}O_{40}]^{3+}$ at 1078 cm^{-1}, 980 cm^{-1}, 898 cm^{-1}, and 796 cm^{-1} were assigned as ν(P-O-W), ν(W=O), ν(W–O–W), and ν(W–O–W), respectively, according to the literature [19]. The solvating water molecules likely contribute to the broad signal that centered about 3100 cm^{-1}.

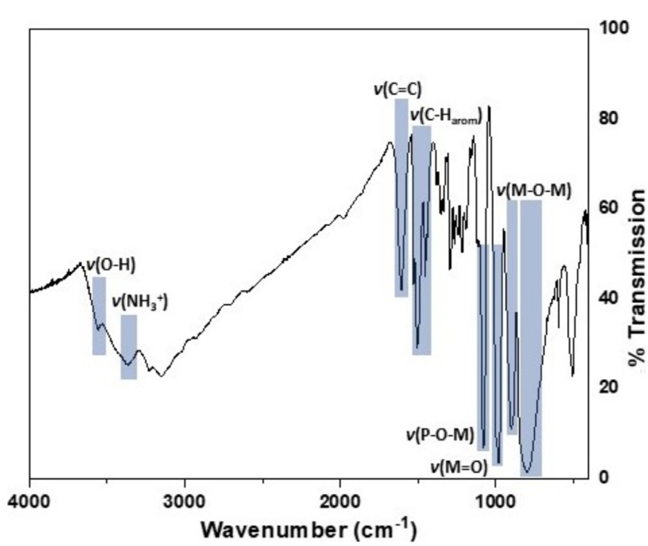

Fig. 3. FTIR spectrum of **1** with key signals highlighted.

3.3. Solution NMR

Crystals of **1** were dissolved in D_2O (~1 mM) and ^1H, ^{31}P and ^1H DOSY NMR spectra were recorded at 37 °C. The ^{31}P NMR spectrum of **1** revealed a major signal at −15.13 ppm, indicating the $[PW_{12}O_{40}]^{3-}$ ion was mostly stable in solution. An additional small signal at ~3 ppm is tentatively ascribed to $[PW_9O_{34}]^{9-}$ [25]. The DOSY experiment with reference dopamine and **1** both gave diffusion constants of 1 • 10^{-9} m^2/s which suggests that dopamine does not interact with $[PW_{12}O_{40}]^{3-}$ ion in aqueous solution to any appreciable extent. These observations are interesting as a previous study found glycine-glycine dipeptide to interact with both $[PW_{12}O_{40}]^{3-}$ and $[PMo_{12}O_{40}]^{3-}$ in D_2O. The $[PW_{12}O_{40}]^{3-}$ ion is known to co-exist in solution with a complex set of equilibrium species, depending on concentration, pH, and counter-ions [25]). Certainly, the current conditions do not reflect the complexity of biological fluids but would still suggest the interaction between phosphotungstic acid and dopamine in aqueous solution is negligible. Adding ~15 mg of **1** to 500 μL Milli-Q H_2O give a pH of about 3.

4. Conclusion

We have herein reported the solid-state structure of the $[HPW_{12}O_{40}(dop)_2]$ complex, which contribute to the structural insight in interactions between biomolecules and nanoparticles. Dopamine interacts with phosphotungstate by hydrogen bonding with its ammonium group in the solid state. However, NMR experiments indicates this complex dissociates in solution.

Declaration of Competing Interest

The authors declare that they have no known competing financial interests or personal relationships that could have appeared to influence the work reported in this paper.

CRediT authorship contribution statement

Fredric G. Svensson: Investigation, Writing - original draft. **Vadim G. Kessler:** Supervision, Writing - review & editing.

Acknowledgements

The support from the Swedish Research Council (Vetenskapsrådet) (grant 2014-3938) is gratefully acknowledged.

Supplementary information

Crystal data can be obtained free of charge from the Cambridge Crystallographic Data Centre via http://www.ccdc.cam.ac.uk/data_request/cif. The CCDC reference number is 2015440.

References

[1] M.F. Hochella, D.W. Mogk, J. Ranville, I.C. Allen, G.W. Luther, L.C. Marr, P. McGrail, M. Murayama, N.P. Qafoku, K.M. Rosso, N. Sahai, P.A. Schroeder, P. Vikesland, P. Westerhoff, Y. Yang, Natural, incidental, and engineered nanomaterials and their impacts on the earth system, Science 363 (2019) 1414.
[2] K.E. Wilkinson, L. Palmberg, E. Witasp, M. Kupczyk, N. Feliu, P. Gerde, G.A. Seisenbaeva, B. Fadeel, S.E. Dahlén, V.G. Kessler, Solution-engineered palladium nanoparticles: model for health effect studies of automotive particulate pollution, ACS Nano 5 (2011) 5312–5324.
[3] V.K. Sharma, J. Filip, R. Zboril, R.S. Varma, Natural Inorganic nanoparticles – formation, fate, and toxicity in the environment, Chem. Soc. Rev. 44 (2015) 8410.
[4] D.M. Smith, J.K. Simon, J.R Baker Jr, Applications of nanotechnology for immunology, Nat. Rev. Immunol. 13 (2013) 592–605.
[5] A.R. Gliga, K. Edoff, F. Caputo, T. Källman, H. Blom, H.L. Karlsson, L. Ghibelli, E. Traversa, S. Ceccatelli, B. Fadeel, Cerium oxide nanoparticles inhibit differentiation of neural stem cells, Sci. Rep. 7 (2017) 9284.

[6] H. Xun, X. Ma, J. Chen, Z. Yang, B. Liu, X. Gao, G. Li, J. Yu, L. Wang, J. Pang, Zinc oxide nanoparticle exposure triggers different gene expression patterns in maize shoots and roots, Environ. Pollut. 229 (2017) 479–488.

[7] A.G. Rodriguez-Campuzano, L.C. Hernandez-Kelly, A. Ortega, Acute exposure to SiO2 nanoparticles affects protein synthesis in Bergmann glia cells, Neurotox. Res. 37 (2020) 366 -39.

[8] H.G.T. Ly, G. Absillis, S.P. Bajpe, J.A. Martens, T.N. Parac-Vogt, Hydrolysis of dipeptides catalyzed by a zirconium(IV)-substituted lindqvist type polyoxometalate, Eur. J. Inorg. Chem. (2013) 4601–4611.

[9] A. Sap, L. Vandebroek, V. Goovaerts, E. Martens, P. Proost, T.N. Parac-Vogt, Highly selective and tunable protein hydrolysis by a polyoxometalate complex in surfactant solutions: a step toward the development of artificial metalloproteases for membrane proteins, ACS Omega 2 (2017) 2026–2033.

[10] G.A. Seisenbaeva, K. Fromell, V.V. Vinogradov, A.N. Terekhov, A.V. Pakhomov, B. Nilsson, K. Nilsson-Ekdahl, V.V. Vinogradov, V.G. Kessler, Dispersion of TiO_2 nanoparticles improves burn wound healing and tissue regeneration through specific interaction with blood serum proteins, Sci. Rep. 7 (2017) 15448.

[11] M.J. Limo, A. Sola-Rabada, E. Boix, V. Thota, Z.C. Westcott, V. Puddu, C.C. Perry, Interactions between metal oxides and biomolecules: from fundamental understanding to applications, Chem. Rev. 118 (2018) 11118–11193.

[12] A. Bijelic, M. Aureliano, A. Rompel, The antibacterial activity of polyoxometalates: structures, antibiotic effects and future perspectives, Chem. Commun. 54 (2018) 1153–1169.

[13] H. Eshtiagh-Hosseini, M. Mirzaei, Two novel chiral inorganic-organic hybrid materials containing preyssler and wells-Dawson heteropolyoxometallates with valine(val), glycine (gly), and proline (pro) amino acids: $(Hval)_2(Hgly)(H_3O)_6K_5[Na(H_2O)P_5W_{30}O_{110}]$.19•5H2O and $(Hpro)_6[P_2W_{18}O_{62}]$.8H2O, J. Clust. Sci. 23 (2012) 345–355.

[14] F.M. Santos, P. Brandao, V. Felix, A.M.V. Cavaleiro, E. de Matos Gomes, M.S. Belsley, Synthesis and structural characterization of Keggin polyoxometalate compounds with argininium(2+) cations, J. Mol. Struct. 963 (2010) 267–273.

[15] M.H. Alizadeh, M. Mirzaei, H. Razavi, 2D-network of inorganic-organic hybrid material built on Keggin type polyoxometallate and amino acid: $[L\text{-}C_2H_6NO_2]_3[(PO_4)Mo_{12}O_{36}].5H_2O$, Mater. Res. Bull. 43 (2008) 546–555.

[16] J. Iijima, H. Naruke, T. Sanji, Chirality induction in crystalline solids containing sandwich-type $[Ln(\alpha_2\text{-}P_2W_{17}O_{61})2]^{17-}$ polyoxotungstates and proline, Inorg. Chem. 57 (2018) 13351–13363.

[17] Z. Han, E. Wang, G. Luan, Y. Li, H. Zhang, Y. Duan, C. Hu, N. Hu, Synthesis, properties and structural characterization of an intermolecular photosensitive complex: (Hgly-gly)3PMo12O40•4H2O, J. Mater. Chem. 12 (2002) 1169–1173.

[18] M. Cindric, T.K. Novak, S. Kraljevic, M. Kralj, B. Kamenar, Strucutral and antitumor activity study of γ-octamolybdates containing aminoacids and peptides, Inorganica Chim. Acta 359 (2006) 1673–1680.

[19] K.M. Rominger, G.N. Nestor, J.E. Eriksson, G.A. Seisenbaeva, V.G Kessler, Complexes of Keggin POMs $[PM_{12}O_{40}]^{3-}$ (M = Mo, W) with GlyGly peptide and arginine – crystal structures and solution reactivity, Eur. J. Inorg. Chem. 2019 (2019) 4297–4305.

[20] C. Hammond, Cellular and Molecular Neurobiology, second ed., Elsevier Science, Burlington, 2012.

[21] T.J. Boyle, T.M. Alam, S.D. Bunge, G.P. Holland, Catechol derivatives of group 4 and 5 compounds, Polyhedron 24 (2005) 1143–1152.

[22] H. Lee, S.M. Dellatore, W.M. Miller, P.B. Messersmith, Mussel-inspired surface chemistry for multifunctional coatings, Science 318 (2007) 426–430.

[23] H. Li, Y. Zhao, Y. Jia, C. Qu, J. Li, Covalently assembled dopamine nanoparticle as an intrinsic photosensitizer and pH-responsive nanocarrier for potential application in anticancer therapy, Chem. Commun. 55 (2019) 15057–15060.

[24] H. Li, Y. Jia, A. Wang, W. Cui, H. Ma, X. Feng, J. Li, Self-assembly of hierarchical nanostructures from dopamine and polyoxometalate for oral drug delivery, Chem. Eur. J. 20 (2014) 499–504.

[25] R.I. Maksimovskaya, G.M. Maksimov, 31P NMR studies of hydrolytic conversions of 12-tungstophosphoric heteropolyacid, Coord. Chem. Rev. 385 (2019) 81–99.